p-Type a-Si:H Doping Using Plasma Immersion Ion Implantation for Silicon Heterojunction Solar Cell Application

Tristan Carrere, Delfina Munoz, Coig Marianne, Christophe Longeaud, Jean-Paul Kleider

p-Type a-Si:H Doping Using Plasma Immersion Ion Implantation for Silicon Heterojunction Solar Cell Application

Tristan Carrere, Delfina Muñoz, Marianne Coig, Christophe Longeaud, and Jean-Paul Kleider*

Plasma immersion ion implantation doping of thin a-Si:H layers is proposed as a new and easy-to-process solution for the fabrication of interdigitated back contacted a-Si/c-Si heterojunction solar cells (SHJ). This study is focused on boron implantation (at low acceleration voltages in the range of 500–1500 V) in a-Si:H layers on a c-Si substrate, to create the strongly doped emitter while maintaining very high c-Si surface passivation, required for high efficiency SHJ solar cells. The influence of implantation parameters and post-annealing temperature on the a-Si:H layer conductivity and passivation quality are assessed. The doped layers conductivity is also investigated by direct and indirect electrical characterization of the density of states in a-Si:H after ion implantation, and the post-implantation annealing. Eventually, an interesting passivation/doping trade-off is obtained after annealing at 300 °C of samples implanted at 1000 V with implied open circuit voltage values of 710 (±5) mV and conductivity values of the doped a-Si:H layer of 3.0 (±1.0) × 10^{-5} Ω^{-1} cm^{-1}, which demonstrates that such approach is promising for processing IBC-SHJ cells.

Introduction: The interdigitated back contact amorphous/crystalline silicon (a-Si:H/c-Si) heterojunction solar cell (IBC-SHJ) is one of the most promising architectures. Indeed, the standard SHJ cell architecture already achieved very high efficiencies (25.1% on large area[1]), and the interdigitated back contact architecture allows to suppress shadowing related to the metallic contacts, thus strongly improving the cells current.[2] Consequently, the IBC-SHJ has recently reached the record efficiency of single-junction silicon solar cells with 25.6%.[3]

However, the patterning of both the hydrogenated amorphous silicon (a-Si:H) and the TCO layers is known to be complex. For instance, processes using sacrificial layers and laser,[4] hard masks and plasma etching,[5] and photolithography[6], have been reported.

Therefore, ion implantation is proposed as a promising solution for amorphous silicon doping. Indeed, three decades ago, the ability of ion implantation to efficiently dope (n)- and (p)-a-Si:H layers has been demonstrated.[7–9] Thus, ion implantation is a promising candidate to decrease manufacturing costs thanks to an easy-to-process solution for localized impurity production with the simple addition of hard masks.

However, the challenge of ion implantation implementation for SHJ cells processing is to maintain a high passivation quality at the critical hetero-interface, despite the very thin a-Si:H layers. A recent study has evidenced strong interface degradations upon beam-line ion implantation (BLII) in thick a-Si:H layers (45 nm).[10] Although optimization of BLII conditions is probably still possible, in this paper, we propose to use a plasma immersion ion implantation (PIII) process where the sample is directly immersed in the precursor gas.[11,12] This configuration allows working at low acceleration energies and is able to shallowly implant the species. Therefore, it appears as a new solution to decrease a-Si:H/c-Si interface damages so that a trade-off between a-Si:H doping and interface passivation quality should be possible.

Using PIII, the goal of this study is to investigate the p-type doping of thin a-Si:H layers (25 nm) for the SHJ cell application, i.e., combining both an efficient (p) a-Si:H doping and a high c-Si substrate passivation.

Materials and methods: 25 nm thick (i) a-Si:H layers are deposited by RF-PECVD on 1 mm thick corning glass and on <100> FZ-grown 180 ± 20 μm thick, 3.0 ± 0.1 Ω cm mirror-like polished 4 inch (n) c-Si substrates. Glass samples are dedicated to a-Si:H layers conductivity measurements, and double side

T. Carrere, D. Muñoz
CEA-INES, LITEN, Laboratoire HET, 50 Avenue du Lac Léman, F-73375 Le Bourget-du-Lac, France
E-mail: delfina.munoz@cea.fr
T. Carrere, C. Longeaud, J.-P. Kleider
GeePs, UMR8507 CNRS, CentraleSupélec, Université Paris-Sud, Université Paris-Saclay, Sorbonne Universités UPMC Univ Paris 6, 11 rue Joliot Curie, F-91192 Gif-sur-Yvette Cedex, France
T. Carrere
French Environment and Energy Management Agency, 20 Avenue du Grésillé BP 90406, F-49004 Angers Cedex 01, France
M. Coig
CEA-LETI, MINATEC Campus, 17 rue des Martyrs, F-38054 Grenoble, France

DOI: 10.1002/solr.201600007

passivated c-Si substrates to lifetime and spectroscopic ellipsometry (SE) measurements.

After deposition, (i) a-Si:H layers are implanted at CEA-Leti using a PULSION® PIII tool. B_2H_6 is used as a precursor gas. Low implantation energies of 500, 1000, and 1500 V and doses of 10^{15}, 5×10^{15}, and 10^{16} cm^{-2} have been tested. The pressure was set to 3.4×10^{-3} mbar, the substrate was maintained at room temperature during implantation, and the implantation time was varied to vary the dose, with a maximum of 300 s for 10^{16} cm^{-2}. It is very unlikely that ions lose energy due to collisions in the sheath, and therefore the ion implantation energy is completely determined by the acceleration voltage over the sheath. Let us note that the dose control system is similar to that of BLII implanters. However, because there is no mass selection, there are many different ionized species implanted and thus the measured charges amount entering the layer does not correspond precisely to the boron (B) dose. Therefore, the real boron dose might be slightly different from the nominal dose. This effect is particularly true for low implantation energies (<1500 V).[13]

Then samples are annealed for 30 min on a hot plate with temperatures ranging from 150 to 300 °C. SE, carrier lifetime and conductivity measurements, are performed after each step ((i) a-Si:H deposition, PIII, cumulative annealing steps). SE measurements are performed using a Jobin-Yvon UVISEL setup and the obtained data are fitted following Tauc Lorenz and using Jellison's approximation.[14] The carrier lifetime is measured using a WCT-120 Sinton Instrument setup[15], while the a-Si:H conductivity is deduced from current–voltage (I–V) measurements on samples on glass where top co-planar Al electrodes were evaporated.

To have a deeper insight into the material and electrical properties, some samples have been submitted to secondary ion mass spectroscopy (SIMS), temperature-dependent photoconductivity and modulated photocurrent (MPC)[16] using a 450 nm illumination with a dc photon flux of 10^{14} cm^{-2} s^{-1}.

Results and discussions. Lifetime measurements: As illustrated in **Figure 1**, lifetimes close to 2 ms are obtained (at an injection level of 10^{15} cm^{-3}) after (i) a-Si:H deposition. After PIII, whatever the implantation conditions, the effective lifetime drops to values lower than 100 µs (Figure 1a). Illiberi et al.[17] conducted Ar^+ implantation experiments at low implantation energy using standard beam-line ion implantation, where the effect of energy was very weak, while the dose had a strong impact.[17] In our case, the decrease is mainly controlled by the implantation energy. The fact that the implantation dose has only a second order influence here (seen for 500 V implantation only) and that B atoms are found at the a-Si:H/c-Si interface in all conditions suggests that the effective lifetime decrease originates from direct implantation damages.

Meanwhile, after annealing, the effective lifetime strongly increases with annealing temperature. The effective lifetime dependence on annealing time has been found logarithmic implying little further recovery after 30 min of annealing, independently of the process conditions. Therefore, a 30 min annealing is performed at each temperature step. For temperatures up to 200 °C, the lifetime recovery rate is lower for samples implanted at higher energies. At temperatures >250 °C, for 1000 and 1500 V implanted samples, passivation recovery after annealing is also improved with increasing the doses. Since a higher dose or a higher implantation energy leads to a higher boron concentration at the a-Si:H/c-Si interface, the results can be explained by an improvement of field-effect passivation provided by the doped a-Si:H region. The fact that this behavior appears at high temperature suggests that an effective doping (i.e., dopant activation) is only obtained at such temperatures. Only samples implanted at the lowest energy succeed to reach an effective lifetime value similar to our (i) a-Si:H/(n) c-Si/(i) a-Si:H reference. It is worth emphasizing that at 300 °C, these samples and the reference exhibit a slight lifetime decrease probably due to hydrogen effusion (the deposition temperature is 200 °C for all layers).[18] All samples have been measured again a few months

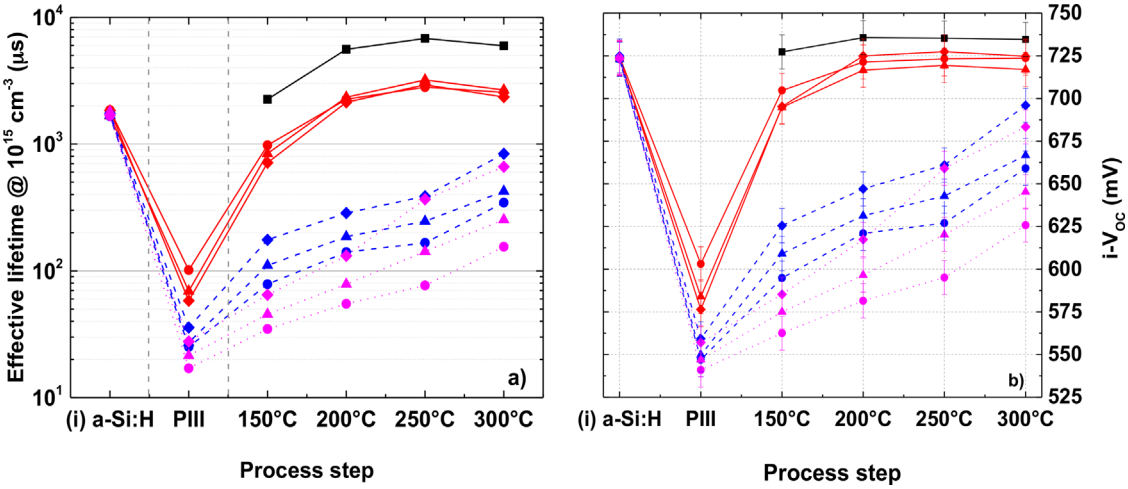

Figure 1. Measured (a) effective lifetime at low injection level (10^{15} cm^{-3}) and (b) 1-sun implied V_{OC} (i-V_{OC}) for samples implanted at different energies (red full lines: 500 V, blue-dashed lines: 1000 V, pink-dotted lines: 1500 V), and doses (●: 10^{15} cm^{-2}, ▲: 5×10^{15} cm^{-2}, ◆: 10^{16} cm^{-2}), and reference sample (black squares) after each process step (a-Si:H deposition, PIII implantation, and cumulative 30 min annealing steps with increasing temperatures).

after implantation and annealing with the reproducible results confirming that such lifetime recovery is a stable mechanism.

Figure 1b shows that an implied-V_{OC} (i-V_{OC}) value of 700 mV is reached for low energy (500 V) implanted samples only. For higher energies, a higher temperature might be able to further improve the passivation recovery up to 700 mV. However, other phenomena such as layers oxidation, stronger H effusion or a-Si:H crystallization could appear above 300 °C and mitigate the beneficial annealing effects.

Conductivity at room temperature: While PECVD deposition results in a homogeneous boron dopant concentration throughout the layer thickness using an ion implantation process leads to non-homogeneous boron profiles. However, SIMS measurements revealed that these non-homogeneous profiles exhibited only small dependence on ion energy, with a characteristic decrease length of about 6 nm. We thus used this value to translate the measured conductance of the samples into an effective conductivity in order to compare the influence of implantation parameters and thermal annealing steps on the transport properties (see **Figure 2**).

As expected, after PIII implantation, the dark room temperature (RT) conductivity is very low ($<10^{-6}\,\Omega^{-1}\,cm^{-1}$). For implantation conditions at 1000 and 1500 V increasing the dose seems to decrease the a-Si:H layer conductivity.

A low temperature (150 °C), annealing tends to decrease the dispersion and gather the samples conductivity between 10^{-9} and $10^{-7}\,\Omega^{-1}\,cm^{-1}$ thus decreasing the conductivity of some samples. A conductivity decrease was already observed after annealing following ion implantation inducing a high amount of damages.[19] Such behavior was linked to a decrease in the density of localized states (DOS) that promote current transport through hopping mechanisms. For our samples, such assertion is supported by the fact that the samples which conductivity is decreased after the 150 °C annealing have been implanted at the higher energies. Therefore, these are the samples with the higher damage content and thus, the higher DOS.

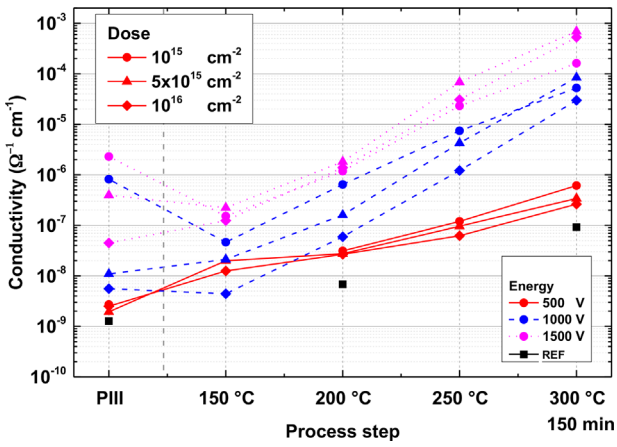

Figure 2. Measured effective room temperature conductivity of (p) a-Si:H layers implanted at different energies and doses (see Figure 1), after each process step: just after implantation (PIII) and after subsequent annealing steps at increasing temperatures (150, 200, 250, and prolonged annealing at 300 °C). For the reference sample, the conductivity before annealing is reported at the PIII step.

Annealing at temperatures above 150 °C increases the conductivities of all samples. As for passivation recovery, the conductivity increase upon annealing is also temperature activated. However, only the samples implanted at 1000 and 1500 V have conductivities surpassing the (i) a-Si:H reference. This indicates either a very low dose of 500 V-implanted dopants (at low acceleration voltage some of the ions may not penetrate into the sample and stay at the surface) or a very small doping efficiency, due to the strong concentration of dopant atoms near the surface (since lower implantation energy leads to thinner depth profile).

The maximum in conductivity is obtained for 1500 V implanted samples and seems to be dose independent. Since the boron depth profiles are very similar after implantation at 1000 and 1500 V, there cannot be a concentration-dependent doping efficiency but it seems that the boron activation upon annealing depends on the implantation energy. As a result, samples implanted at 1500 V and at doses of 5×10^{15} and $10^{16}\,cm^{-2}$ succeed to reach conductivities above $10^{-4}\,\Omega^{-1}\,cm^{-1}$ (currently used for SHJ cells[18]), compared to $10^{-2}\,\Omega^{-1}\,cm^{-1}$ already achieved using BLII implantation and with a similar average boron concentration ($[B]\sim10^{22}\,cm^{-3}$).[20]

To explain this difference, one can first note that implanted dopant activation is lower than in PECVD-doped layers.[20] Moreover, the activation difference with Le Comber's experiment might originate from the PIII parasitic implantation of C and F atoms that is revealed from SIMS measurements. They are known to decrease the a-Si:H layer conductivity and act as n-type doping, respectively.[9,21] Finally, the implantation doses and energies and the a-Si:H layer thickness are very different from literature experiments, since the latter targeted thin film a-Si:H solar cell applications.

Doping/passivation discussions: Because of a higher doping species activation efficiency and enhanced damages with higher ion implantation energies, we observe a trade-off between passivation and doping. At first sight the higher the energy, the higher the conductivity and the lower the passivation recovery.

The control of both the passivation and the conductivity by the ion implantation energy (Figures 1 and 2) is quite surprising compared to literature results, that rather report a control of doping by the ion dose.[7,19,20,22] These differences might originate from the much higher a-Si:H layer thickness of literature studies (~100 nm) and the very different implantation parameters. The observed evolution of our samples properties upon temperature annealing might be related to changes in the hydrogen configuration. However, no obvious change was observed in the absorption spectra from Fourier Transform InfraRed spectroscopy performed before and after annealing.

A complementary test with a prolonged 300 °C annealing for 2 h 30 min has also been performed in order to further benefit from the 300 °C annealing for both the doping and passivation properties. Such prolonged annealing succeeded in slightly increasing the conductivity and the lifetime of 1000 and 1500 V-implanted samples. The best results have been obtained for a trade-off with an i-V_{OC} value of 710 ± 5 mV and an effective conductivity value of $3\pm1\times10^{-5}\,\Omega^{-1}\,cm^{-1}$ for the 1000 V – $1\times10^{16}\,cm^{-2}$ sample.

MPC measurements: **Figure 3** introduces the MPC[16] measurement results of the samples implanted at 500 V and

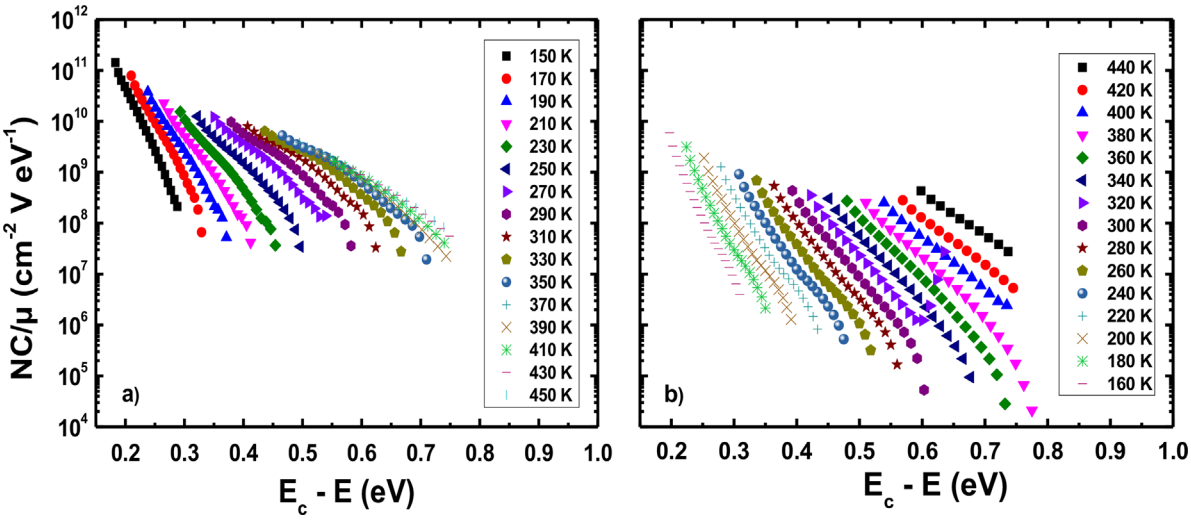

Figure 3. MPC measurement results of a-Si:H layer with a B_2H_6-PIII at 500 V and 10^{16} cm^{-2} (a) after PIII and (b) after PIII and annealing at 440 K for 60 min.

10^{16} cm^{-2} after the implantation step. The graph displays the NC/μ ratio calculated in the high frequency MPC regime assumption for various temperatures and 21 frequencies (ranging from 12 Hz to 39.9 kHz in geometric progression), N being the DOS, C the capture coefficient, and μ the mobility of the carriers, that give the major contribution to the modulated photocurrent, as a function of the energy in the gap referred to the band edge. Due to the larger valence band tail compared to the conduction band tail, and to lower mobility of holes compared to that of electrons in a-Si:H, it is likely that the probed states in the high frequency regime of MPC are electron trapping states, thus explaining that the energy scale has been referred to the conduction band edge.

After PIII, the NC/μ values at different temperatures overlap at high frequency (i.e., lowest E_c-E values at each temperature). The overlapped regions forming the upper envelope can be considered as representative of the DOS shape in the material. The absolute value of NC/μ (10^{11} cm^{-2} V eV^{-1} at 0.2 eV) is much higher than for intrinsic samples reported in literature (by two orders of magnitude).[23,24] This primarily indicates that PIII implantation in a-Si:H induces a high density of localized states that can prevent the Fermi level from moving close to the valence band, thus leading to a poor doping effect.

After annealing, a strong decrease of NC/μ value (about two orders of magnitudes) is observed, which indicates a significant decrease in the localized density of states upon annealing. The shape of the curves has also changed and the overlap of the curves at high frequency is mainly lost, which points toward strong changes in the microstructure of the material, like a possible partial crystallization and/or doping activation together with a reduction in defect density (C. Longeaud, private communication), although we could not find a proof of crystallization from spectroscopic ellipsometry and Raman measurements.[25]

This result is a direct observation of DOS evolution in ion implanted a-Si:H layers, and confirms indirect observations of DOS decrease upon annealing, characterized by photo-conductance. It is also consistent with previous works in literature that indirectly observed that (i) ion implantation introduces a large amount of localized defects in a-Si:H, due to structural defects (dangling bonds, floating bonds, strained Si—Si bonds, vacancy-like defects)[26], and (ii) the increase in samples conductivity upon annealing originates from a defect recovery.[19,27]

Dark- and photo-conductivity: In order to further support the latter DOS behavior analysis, the 500 V and 10^{16} cm^{-2} implanted samples have been also characterized by means of dark- and photo-conductivity (DC and PC, respectively), as a function of temperature (**Figure 4**a). The temperature is first increased from 110 to 450 K, a 450 K annealing is performed for 30 min, and the temperature is then decreased from 450 to 110 K. First it is observed that the DC has an activated behavior above 300 K and the corresponding activation energy decreases from 1.0 to 0.6 eV after the 450 K annealing step, revealing a clear shift of the Fermi level. Moreover, the PC at and below room temperature is increased by more than two orders of magnitude after annealing. Since deep-localized states act as recombination centers for excess carriers,[27] this behavior supports the DOS evolution observed from MPC in the previous section. One can also note a slight PC increase when sweeping from high to low temperature. Such behavior is probably related to the activation of localized defects with softer recombination parameters (i.e., lower capture cross sections).

The photosensitivity after each process step is presented in Figure 4b. It is decreased after the PIII step, validating the increase in the DOS after PIII. Stronger implantation energies lead to stronger damages (i.e., higher DOS), and thus, to a stronger photosensitivity decrease. After annealing at 150 °C, the photosensitivity increases because of the DOS decrease. Such DOS recovery is higher for the more lowly damaged samples (i.e., those implanted at lower energies). Finally, at higher annealing temperatures the photosensitivity decreases again, which may be related to the dopant activation, leading to an increase of the dark conductivity (see Figure 2).

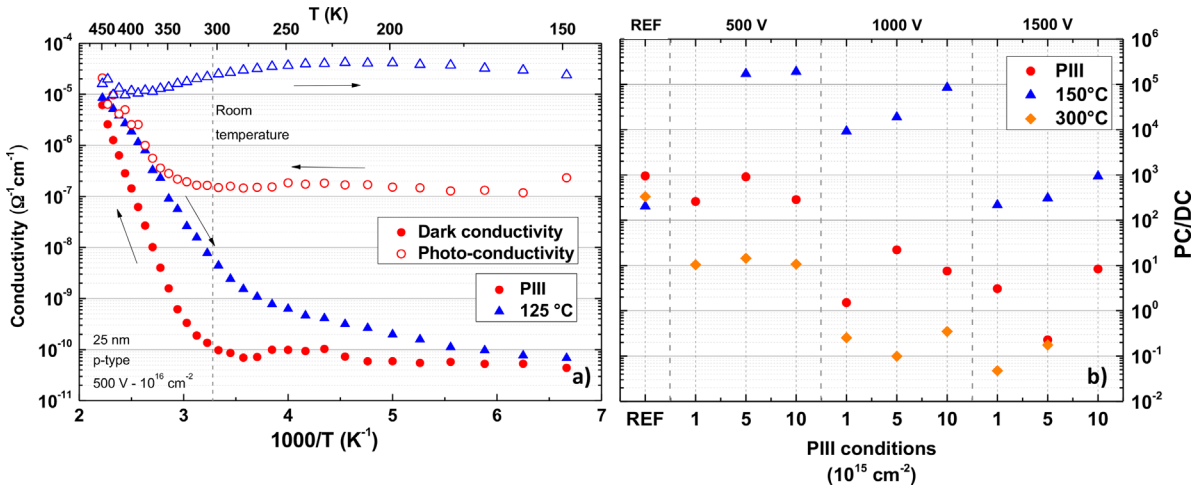

Figure 4. (a) Dark- (DC) and photo (PC)-conductivity measurement after a 500 V and 10^{16} cm^{-2} PIII B_2H_6 implantation against temperature. (b) Room temperature photosensitivity after each process step and against different PIII implantation conditions. For this latter experiment only, a 630 nm illumination at a flux of 2.6×10^{16} cm^{-2} s^{-1} is used.

As a result, the analysis of the photo-conductivity and photosensitivity behavior are well correlated to the MPC results and suggest changes in the DOS after PIII and subsequent annealing steps.

Conclusion: In this work, the doping/passivation trade-off of boron-implanted thin a-Si:H layers has been investigated.

After plasma immersion ion implantation, conductivities of a-Si:H layers and effective lifetimes of a-Si:H/c-Si/a-Si:H samples are very low, due to a poor doping activation and strong a-Si:H/c-Si interface damages. A post-implantation hot plate annealing is successfully used to recover (at least partially) both properties. After annealing samples implanted at higher energies exhibit higher conductivities. The conductivity increase is directly (from MPC) and indirectly (from dark- and photo-conductivity) observed to originate from a strong decrease of the density of states in a-Si:H. Field-effect passivation is also evidenced for layers exhibiting a high conductivity.

Promising results have been achieved using PIII acceleration voltage of 1000 V and implanted dose of 1×10^{16} cm^{-2}, with a-Si:H layers exhibiting reasonable room temperature conductivity, $\sigma_{RT} = 3 \pm 1 \times 10^{-5}\ \Omega^{-1}\,\text{cm}^{-1}$, and leading to high implied open circuit voltage, i-$V_{OC} = 710 \pm 5$ mV, after prolonged annealing at the highest tested annealing temperature (150 min at 300 °C).

The monotonous increase of passivation and doping properties with annealing temperature suggests that higher temperature should provide improved layer properties. Therefore, together with a finer implantation parameters tuning, there is space for promising improvements. The doping of (p) a-Si:H layers now appears as a very promising way of processing IBC-SHJ solar cells.

Acknowledgements

The authors would like to acknowledge F. Milesi and P. Mur from CEA Léti for all the ion implantation processes. They also thank the French Environment and Energy Management Agency (ADEME) and the French Alternative Energies and Atomic Energy Commission (CEA) for funding this work. This study was also supported by the European Union through the HERCULES project that has received funding from the European Union's Seventh Programme for research, technological development, and demonstration under grant agreement no. 608498.

Received: November 5, 2016
Revised: December 18, 2016
Published online: February 7, 2017

[1] Adachi, D., Hernández, J. L., Yamamoto, K., *Appl. Phys. Lett.* **2015**, *107*, 233506.
[2] Green, M. A., Emery, K., Hishikawa, Y., Warta, W., Dunlop, E. D, *Prog. Photovoltaics Res. Appl.* **2016**, *24*, 905.
[3] Masuko, K., Shigematsu, M., Hashiguchi, T., Fujishima, D., Kai, M., Yoshimura, N., Yamaguchi, T., Ichihashi, Y., Mishima, T., Matsubara, N., Yamanishi, T., Takahama, T., Taguchi, M., Maruyama, E., Okamoto, S., *IEEE J. Photovolt.* **2014**, *4*, 1433.
[4] Desrues, T., De Vecchi, S., d'Alonzo, G., Munoz, D., Ribeyron, P.-J., Influence of the emitter coverage on interdigitated back contact (IBC) silicon heterojunction (SHJ) solar cells, in *IEEE 40th Photovoltaic Specialists Conference*, Denver, **2014**, p. 857.
[5] Paviet-Salomon, B., Tomasi, A., Descoeudres, A., Barraud, L., Nicolay, S., Despeisse, M., De Wolf, S., Ballif, C., *IEEE J. Photovolt.* **2015**, *5*, 1293.
[6] Nakamura, C., Asano, N., Hieda, T., Okamoto, C., Katayama, H., Nakamura, K., *IEEE J. Photovolt.* **2015**, *4*, 1491.
[7] Müller, G., Kalbitzer, S., Spear, W. E., Le Comber, P. G., Doping of amorphous silicon by ion implantation, in *7th International Conference on Amorphous and Liquid Semiconductors* **1977**, edited by W. E. Spear (CICL, University of Edinburgh), p. 442.
[8] Spear, W. E., Le Comber, P. G., Kalbitzer, S., Mueller, G., *Philos. Mag. B* **1979**, *39*, 159.
[9] Kalbitzer, S., Mueller, G., Le Comber, P. G., Spear, W. E., *Philos. Mag. B* **1980**, *41*, 439.
[10] Defresne, A., Plantevin, O., Sobkowicz, I. P., Bourçois, J., Roca. i Cabarrocas, P., *Nucl. Instr. Meth. B* **2015**, *365*, 133.
[11] Torregrosa, F., Laviron, C., Faik, H., Barakel, D., Milesi, F., Beccaccia, S., *Surf. Coat. Technol.* **2004**, *186*, 93.
[12] Etienne, H., Vervisch, V., Torregrosa, F., Sarnet, T., Delaporte, P., Cristiano, F., Fazzini, P. F., Roux, L., Sempere, G., Ultra shallow

junctions fabrication by Plasma Immersion Implantation on PULSION® followed by different annealing processes, in *Extended Abstracts — 2008 8th International Workshop on Junction Technology (IWJT '08)* **2008**, p. 32.
[13] Felch, S. B., Fang, Z., Koo, B.-W., Liebert, R. B., Walther, S. R., Hacker, D., *Surf. Coat. Technol*. **2002**, *156*, 229.
[14] Jellison, J. G. E., Modine, F. A., *Appl. Phys. Lett*. **1996**, *69*, 371.
[15] Sinton, R. A., Cuevas, A., Stuckings, M., Quasi-steady-state photoconductance, a new method for solar cell material and device characterization, in 25th IEEE Photovoltaic Specialists Conference, Washington DC, **1996**, p. 457.
[16] Kleider, J.-P., Longeaud, C. Gueunier, M.-E., *Phys. Status Solidi (C)* **2004**, *1*, 1208.
[17] Illiberi, A., Kudlacek, P., Smets, A. H. M., Creatore, M., van de Sanden, M. C. M., *Appl. Phys. Lett*. **2011**, *98*, 242115.
[18] De Wolf, S., Kondo, M., *Appl. Phys. Lett*. **2007**, *91*, 112109.
[19] Müller, G., Le Comber, P. G., *Philos. Mag. B* **1981**, *43*, 419.
[20] Le Comber, P. G., Spear, W. E., Müller, G., Kalbitzer, S., *J. Non Cryst. Solids* **1980**, *35*, 327.
[21] Zhang, D., Deligiannis, D., Papakonstantinou, G., van Swaaij, R. A., Zeman, M., *IEEE J. Photovolt*. **2014**, *4*, 1326.
[22] Van Der Weg, W. F., Berntsen, A. J. M., Saris, F. W., Polman, A., *Mater. Chem. Phys*. **1996**, *46*, 140.
[23] Luckas, J., Longeaud, C., Siebentritt, S., *J. Appl. Phys*. **2014**, *116*, 103710.
[24] Longeaud, C., Schmidt, J., Koropecki, R. R., Kleider, J.-P., *J. Optoelectron. Adv. Mater*. **2009**, *11*, 1064.
[25] Shahidul Haque, M., Naseem, H. A., Brown, W. D., *J. Appl. Phys*. **1994**, *75*, 3928.
[26] Coffa, S., Priolo, F., Battaglia, A., *Phys. Rev. Lett*. **1993**, *70*, 3756.
[27] Galloni, R., Tsuo, Y. S., Baker, D. W., Zignani, F., *Appl. Phys. Lett*. **1990**, *56*, 241.